ХОЛОДИЛЬНА ТЕХНІКА ТА ЕНЕРГОТЕХНОЛОГІЇ

УДК: 62-717

Numerical simulation of the regime and geometric characteristics influence on the pressure loss of a low-flow aerothermopressor

D. Konovalov [1] ✉, ***H. Kobalava*** [2]
Admiral Makarov National University of Shipbuilding, Kherson branch, Ushakov Avenue, 44, Kherson, 73003, Ukraine
✉ e-mail: dimitriyko79@gmail.com,
ORCID ID: [1] https://orcid.org/0000-0001-7127-0487, [2] https://orcid.org/0000-0002-0634-5814

In this paper, a study of gasdynamic processes that occur in a low-flow aerothermopressor has been done. The aerothermopressor is a two-phase jet apparatus for contact cooling, in which, due to the removal of heat from the air flow, the air pressure is increased (thermogasdynamic compression) and its cooling is taken place. Highly effective operation of the aerothermopressor is influenced by primarily the flow part design and the water injected method in the apparatus. Constructive factors that influence energy costs to overcome friction losses and local resistances on the convergent-divergent sections of the aerothermopressor are exerted a significant impact on the working processes in the apparatus. In this paper, a study of a number of typical low-flow aerothermopressor models has been conducted by using computer CFD modeling. Determination of the main parameters of the air flow (total pressure, dynamic pressure, velocity, temperature, etc.) has been carried out for a number of taper angles of a confuser α and a diffuser β, as well as for a number of values of the relative air velocity in the working chamber M = 0.4-0.8. Comparison of the obtained data with experimental data has been carried out. The deviation of the calculated values of local resistances coefficients in the confuser and in the diffuser from those obtained by computer CFD modeling does not exceed 7–10%. The recommended angles were determined: confuser convergent angle – 30° and diffuser divergent angle – 6°, corresponding to the minimum pressure loss is 1.0 – 9.5 %, and therefore also to the maximum pressure increase as a result of the thermogasdynamic compression that occurs during injection and evaporation of liquid in the working chamber. Thus, analytical dependences are obtained for determining the local resistance coefficients for the confuser (nozzle) and the diffuser, which can be recommended to use in the design methodology for low-flow aerothermopressors.

Keywords: *Aerothermopressor, Coefficients of local resistance, CFD modeling*

doi: https://doi.org/10.15673/ret.v55i2.1355

1. Introduction

Jet devices have long taken their place in the technical area and are widely used, both as individual devices, and as part of power plants to improve cooling systems and to increase fuel and energy efficiency. An aerothermopressor is one of such devices, it is a two-phase jet apparatus for contact cooling, in which, due to the removal of heat from the air flow, the air pressure is increased (thermogasdynamic compression) and its cooling is taken place.

The aerothermopressor effectiveness depends on the values of total pressure losses due to the following factors: surface and internal friction of the air, aerodynamic resistance of the injection system, resistance of the injected liquid, the process of heat and mass transfer at a finite temperature difference and partial pressure. Such losses can be quite significant and amount to 10-40%, depending on the design features of the apparatus flow-through part.

Therefore, taking this into account, the actual development of the aerothermopressor type jet technology is the determination of rational parameters of the workflow organization with the corresponding development of the flow part design. At the same time, it is necessary to have an opportunity for the analytical determination of losses associated primarily with friction in the confuser (nozzle) and diffuser of the aerothermopressor.

Use of the low-flow aerothermopressor in the cycle air cooling system of low-power gas turbines (microturbines) is highly topical issue.

2. Literature Review

The aerothermopressors using as contact heat exchangers is possible for a wide range of power plants, namely for cooling the cycle air of gas turbines of various nominal capacities [1], cooling the charge air of internal combustion engines [2], for removing superheating of vapor in industrial ammonia two-stage refrigeration plants of moderate cold [3], etc. Due to the evaporative cooling in the aerothermopressor, the effect of thermogasdynamic compression takes place, that is, an increase in air pressure, as a result of the instantaneous evaporation of water, which is injected into the accelerated hot air flow. The heat that goes to the evaporation of water is taken from the air flow, thereby cooling it.

To ensure the highly efficient operation of the aerothermopressor, it is necessary to determine the technological requirements for the flow part design and the water injected method in the apparatus. A significant influence on the working processes in the aerothermopressor is exercised by design factors that influence energy costs to overcome the friction losses and local resistances on the convergent-divergent sections of the aerothermopressor.

The air velocity at the minimum cross-section of the aerothermopressor should be M = 0.5-0.9 to ensure a positive increase in pressure. At such a velocity, the total pressure loss is increased rapidly [4].

Pressure losses due to aerodynamic resistance in the flow-through part of the aerothermopressor are determined by the local resistance coefficients: confuser (nozzle) – ζ_c; working chamber (evaporation area) – ζ_{ch}; diffuser – ζ_d.

The well-known classical methods of hydrodynamics and fluid flow mechanics are used to calculate losses from the total resistance [5, 6, 7, 8]. So to determine the coefficients of the total hydraulic resistance of the confuser (1) and diffuser (2) the following dependencies are used [5, 6, 8]:

$$\zeta_c = \left(\frac{\lambda_c}{8 \sin \frac{\alpha}{2}} \right) \cdot \left(1 - \left(\frac{d_{ch}^4}{d_c^4} \right) \right), \qquad (1)$$

$$\zeta_d = \left(\frac{\lambda_d}{8 \sin \frac{\beta}{2}} \right) \cdot \left(1 - \left(\frac{d_{ch}^4}{d_d^4} \right) \right) + \sin \beta \cdot \left(1 - \frac{d_{ch}^2}{d_d^2} \right)^2, \qquad (2)$$

where λ_c – average value of hydraulic friction coefficients at the beginning and at the end of the confuser; α – confuser taper angle, °; d_c – confuser diameter, m; d_{ch} – working (evaporation) chamber diameter, m; λ_d – average coefficient of hydraulic friction at the beginning and at the end of the diffuser; β – diffuser taper angle, °; d_d – diffuser diameter, m.

When the air velocity is M = 0.5-0.7, the resistance coefficient for the working chamber ζ_{ch} resides in the region of the self-similar air flow according to the Reynolds number (Re) and the Mach number (M). Depending on the degree of roughness of the walls, ζ_{ch} can be defined as [4]:

$$\zeta_{ch} = (0.01 - 0.02) \frac{L_{ch}}{D_{ch}} \qquad (3)$$

(L_{ch}/D_{ch}) – caliber or relative diameter - the ratio of the length of the mixing chamber to its diameter.

To determine the coefficient of local resistance of the diffuser ζ_d, there are two main methods: semi-empirical and based on the boundary layer theory.

The disadvantage of the semi-empirical method is that it does not take into account the effect of gas compressibility, operating parameters in the minimum cross section and the conditions of entry and the initial stage of flow turbulence. This, in turn, gives the value of ζ_d several times different from the real (experimental) value [4, 9].

In the method of determining ζ_d, on the basis of the theory of the boundary layer, the integral characteristics of the boundary layer are determined and, on their basis, analytical dependences are obtained for the calculation. The disadvantage of this method is the need to satisfy the condition of uniformity of the velocity field at the entrance, which is very difficult to obtain in practice [9].

The above methods for determining local resistance coefficients do not provide accurate data on losses in the diffuser, which, in turn, makes it necessary to use the data obtained during the experiment [4] in studies in a wide range of geometric and regime parameters.

It should be noted that with Reynolds numbers $Re \le 2 \cdot 10^5$ the local resistance coefficient does not depend on the Reynolds Re number and the Mach number M (in the range of values M = 0.1-0.9) and is determined only by geometrical parameters (for example, the angle of tapering and the ratio of the diameters of the input and output D_1/D_2). Considering the above, it has been established that the value of the local resistance coefficient resides in the region of the self-similar flow regime for Re and M [4], that is, the air flow remains mechanically similar to itself when one or several parameters determine this flow change.

The smallest value ζ_d = 0.06-0.08 corresponds to the angle of the diffuser expansion β = 5-7 ° and the degree of expansion n = 10. The above data are valid provided that the velocity field at the input [4] is uniform. If there is a working chamber in front of the diffuser with a sufficiently large caliber value (L_{ch}/D_{ch}), the velocity distribution field will be substantially uneven. The value of ζ_d can be calculated by the following equations [5]:

$$\zeta_{un} = K \cdot \zeta_d , \quad (4)$$

K – correction factor.

When $Re > 10^5$ i $(L_{ch}/D_{ch}) = 5\text{-}15$, the value of the correction factor can be taken K = 1.3-1.6. Thus, the value of the local resistance coefficient will be $\zeta_d = 0.08\text{-}0.15$.

A study was made [10] of the aerothermopressor operation on the exhaust gases of a gas turbine. The authors designed and investigated an experimental jet apparatus, 7.5 meters long, an initial flow velocity was equal to 31 m/s, the gas flow rate was equal to 11.5 kg/s. The data on pressure loss through local and hydraulic resistance in different parts of the aerothermopressor were obtained, the total pressure resistance without fluid injection reached 14 %.

In the works [1, 11] it is shown that the positive effect from the thermogasdynamic compression use in the aerothermopressor (increasing the air pressure during cooling) is greater, then the friction loss is smaller. Losses due to friction according to the classical method of calculation are up to 5-8 %.

The discrepancy of theoretical data, based on classical dependencies, and experimental data indicates inaccuracy in determining local coefficients of pressure loss, which is especially important with small diameters of the flow-through part of the aerothermopressor, that is, with low air flow.

Obviously, to determine losses from the total resistance in the low-flow aerothermopressor (air flow G_{air} is up to 1 kg/s), it is necessary to clarify the empirical dependences to determine the coefficients of total aerodynamic resistance through the small diameters of the apparatus flow part. The establishment of such dependences or a range of specific values for local coefficients of pressure loss will allow choosing the optimal structural characteristics of the aerothermopressor, which will correspond to the achievement of the maximum pressure increase value as a result of thermogasdynamic compression.

The study purpose is to obtain analytical dependencies for determining the local resistance coefficients for the confuser and the diffuser of the low-flow aerothermopressor.

3. Research Methodology

To determine the optimal design parameters of the experimental aerothermopressor (Fig. 1) at various air flow rates in the working chamber (M = 0.4–0.8), a hydrodynamic analysis of typical models was carried out by using CFD modeling software ANSYS Fluent [12].

The experimental aerothermopressor was developed to study the working processes with the thermogasdynamic compression emergence in order to determine the optimal geometrical and regime parameters. The working medium is humid air with initial parameters of pressure P_{atp1}, temperature T_{atp1} and relative humidity φ_{atp1}, corresponding to the parameters of the cycle air of gas turbines and charge air of internal combustion engines (Table 1).

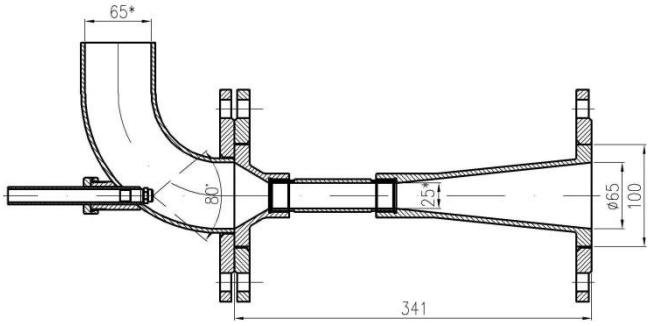

Figure 1 *– The design of the experimental aerothermopressor*

Table 1 – Technical characteristics of the experimental aerothermopressor

Parameter	Value
Inlet air pressure P_{atp1}, 10^5 Pa	3.0
Inlet air temperature T_{atp1}, K	453
Relative inlet humidity φ_{atp1}, %	30
Air velocity at the inlet confuser (nozzle) w_{air1}, m/s	35
Mach number at the inlet working chamber M	0.40–0.80
Relative velocity of injected fluid (w_w/w_{air1})	0.3
Temperature of injected fluid T_{w1}, K	293
Air mass flow G_{air}, kg/s	0.34
Relative mass flow rate of injected fluid g_w, %	5

To build a three-dimensional solid model, AutoCAD graphic program was used (Fig. 2). The input and output sections of the geometric model were elongated to eliminate the influence of edge effects in the computational model. The geometrical characteristics of the aerothermopressor were given in Table 2.

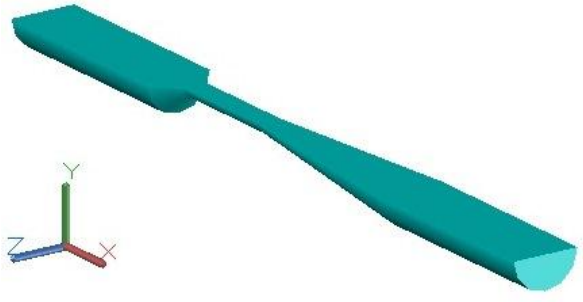

Figure 2 *– 3D model of the experimental aerothermopressor*

Table 2 – Flow part geometric characteristics of the experimental aerothermopressor

Parameter	Dimension
Aerothermopressor length L_{atp}, mm (L_{ch}/D_{ch}) = 5	341
Confuser	
Inlet diameter D_{c1}, mm	64
Outlet diameter D_{c2}, mm	22
Angle α, °	30; 35; 40; 45; 50
Length L_c, mm (at α = 30 °)	36
Diffuser	
Inlet diameter D_{d1}, mm	22
Outlet diameter D_{d2}, mm	65
Angle β, °	6; 8; 10; 12
Length L_d, mm (at β = 6 °)	208
Working chamber at (L_{ch}/D_{ch}) = 5	
Diameter D_{ch}, mm	22
Length L_{ch}, mm	108

The computational grid (Fig. 3) was constructed by using the Automatic Method, the grid elements are tetrahedrals. The maximum size of each element does not exceed 3 mm. Wall layers are specified in the amount of 4 pieces (Table 3).

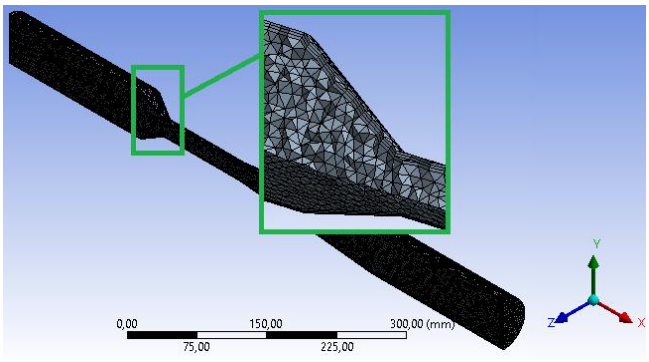

Figure 3 *– Computational grid for modeling of the experimental aerothermopressor*

Table 3 – Calculation grid parameters for modeling of the experimental aerothermopressor

Parameter	Value
Amount of nodes	70575
Amount of elements	290890
Thickness of the first wall layer, mm	0.5
Amount of wall layers	4
Maximum mesh size, mm	3.0

Numerical simulation of the airflow process in the aerothermopressor was carried out using the finite volume method in the ANSYS Fluent software package. A calculation method was defined based on the Pressure-Based solvers, a turbulence model was selected, a calculation was made taking into account the convergence of results, and the output data were processed and visualized in Postprocessing in the form of graphs, fields and streamlines for the main parameters of the workflow. The calculation of the air flow parameters (total pressure, dynamic pressure, velocity, temperature, etc.) in the aerothermopressor was carried out for a number of confusor and diffuser taper angles, as well as for a number of relative air velocity values in the working chamber M = 0.4-0.8.

To study of the air flow behavior, k-ε Realizable two-parameter turbulence model was used from the group of models Reynolds-Averaged Navier-Stokes (RANS). This model is recommended for axisymmetric flows in jet devices and makes it possible to predict the behavior of the flow propagation velocity and has proven itself in solving engineering problems [13, 14, 15, 16].

To determine the local resistance coefficients for the diffuser and confuser, classical dependences of fluid dynamics [5, 6] were used.

The energy equation (Bernoulli equation for air flow, taking into account mechanical specific losses):

$$\rho g z_1 + p_1 + N_1 \frac{\rho w_1^2}{2} = \rho g z_2 + p_2 + N_2 \frac{\rho w_2^2}{2} + \Delta p_t, \quad (5)$$

where $\rho g z_1$, $\rho g z_2$ – geometric pressure, Pa; p_1, p_2 – static pressure, Pa; Δp_t – total losses of total pressure, Pa; $N_1 \frac{\rho w_1^2}{2}$, $N_2 \frac{\rho w_2^2}{2}$ – dynamic pressure, Pa.

Dividing by ρg:

$$z_1 + \frac{p_1}{g\rho} + N_1 \frac{w_1^2}{2g} = z_2 + \frac{p_2}{g\rho} + N_2 \frac{w_2^2}{2g} + \Delta h_t, \quad (6)$$

Δh_t – total head losses, m.

The equation for total pressure is:

$$p_t = p_1 + N_1 \frac{\rho w_1^2}{2} \quad (7)$$

Taking into account the fact that $z_1 = z_2$ and Eq. (7), the total head losses Δh_t:

$$\Delta h_t = \frac{p_{t1} - p_{t2}}{g\rho} \quad (8)$$

The local resistance coefficient ζ_t is:

$$\zeta_t = \frac{2\Delta p_t}{\rho w^2} \quad (9)$$

To check the adequacy of the obtained analytical dependencies for the local resistance coefficients, the experimental data given in [4, 9, 17] were used. The experimental data were compared with those ob-

tained during CFD modeling and their relative discrepancy was determined.

4. Results and Discussions

According to the results of computer CFD modeling of models of the aerothermopressor, the value of local resistance coefficients for the diffuser (divergent angle $\beta = 6; 8; 10; 12°$) and confuser (convergent angle $\alpha = 30; 35; 40; 45; 50°$). Initial data at the confuser part inlet of the aerothermopressor: $P_1 = 3 \cdot 10^5$ Pa; $T_1 = 453$ K, $w_{air} = 35$ m/s. It should be noted that the nature of the change in air velocity w_{air} along the length of the flow part is fairly uniform (Fig. 4), and the velocity profiles change almost proportionally (Fig. 5).

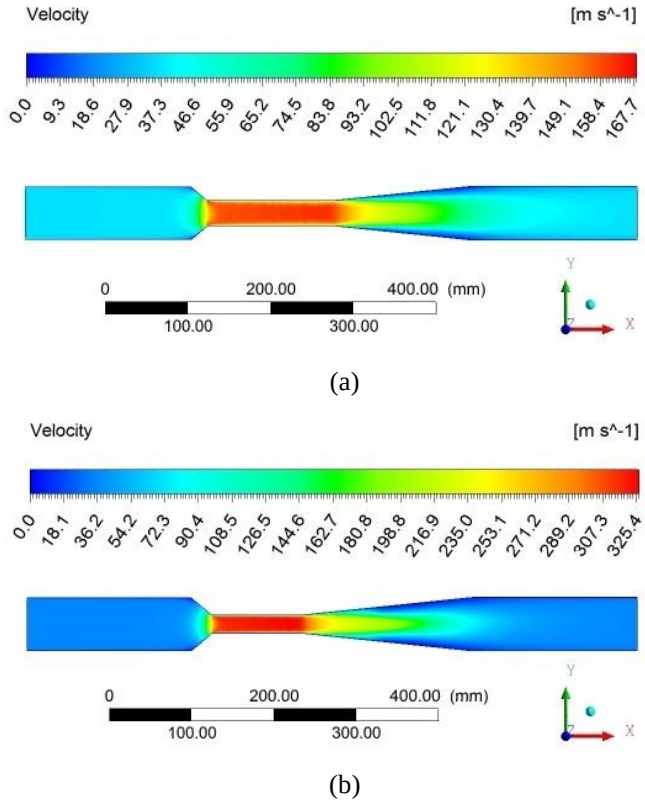

Figure 4 *– Velocity field distribution in the flow part of the aerothermopressor at the inlet velocity to the working chamber M = 0.4 (a) and M = 0.8 (b)*

In addition, the value of local resistance coefficients, both for the confuser ζ_c and for the diffuser ζ_d, practically do not change when the velocity in the working chamber M = 0.4–0.8 (Fig. 6) and Re average value change (Fig. 7). At the same time, for confuser – $\zeta_c = 0.02–0.08$, where lower values correspond to the convergent angle $\alpha = 30$ °. The influence of the diffuser resistance is more significant – $\zeta_d = 0.08–0.32$, where the diffuser with the divergent angle $\beta = 6$ ° has a smaller value. The absence of the influence of Re and M on ζ_c and ζ_d indicates that there is a self-similar flow regime both in the confuser and in the diffuser of the aerothermopressor, that is, the value of the local resistance coefficient depends only on the geometric parameters (opening angle α and β, expansion n_d and contraction n_c ratio) of the corresponding channel.

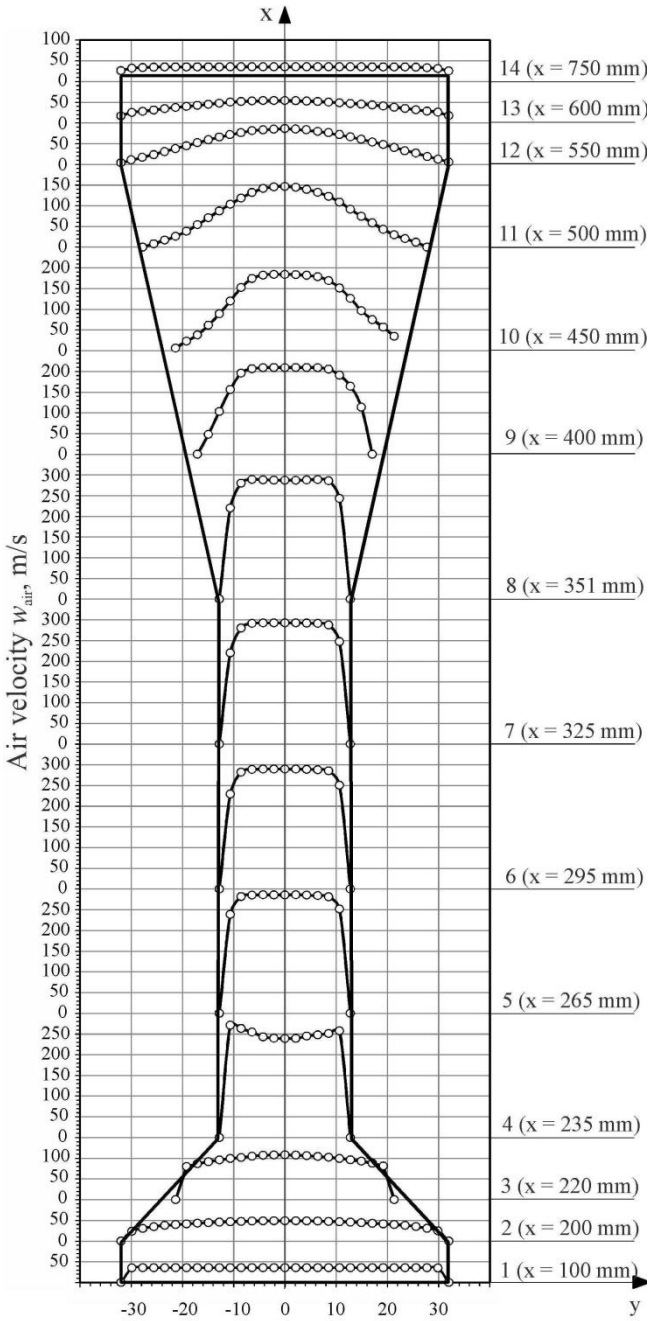

Figure 5 *– Velocity diagrams distribution over the sections of the flow-through part of the aerothermopressor: $\alpha = 30$ °; $\beta = 6$ °; M = 0.6; $n_c = 6.6$; $n_d = 6.8$; $G_{air} = 0.34$ kg/s; x - distance from the inlet part aerothermopressor*

Considering the above, the equation determination for the coefficient of local resistance of the confuser ζ_c was carried out by the method of approximation depending on the geometric parameters in accordance with a number of equations. In this case, the equations of a paraboloid of rotation were chosen (Fig. 8):

$$z = y_0 + ax + by + cx^2 + dy^2 \quad (10)$$

or

$$\zeta_c = \sin\alpha\left(0.3287\sin\alpha - 0.2421\right) + \\ + n_c\left(7\cdot10^{-4}n_c - 0.0063\right) + 0.0858 \quad (11)$$

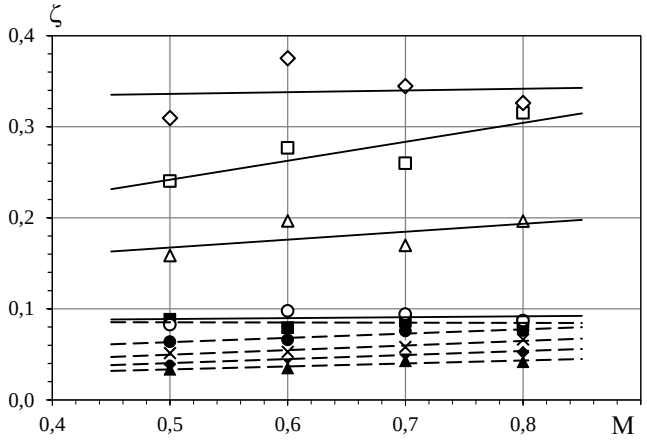

Figure 6 *– Dependence of local resistance coefficients ζ on the velocity M at the inlet to the working chamber:*

_____ - diffuser; _ _ _ _ - confuser; diffuser divergent angle: ○ - 6 °; △ - 8 °; □ - 10 °;◇ - 12 °; confuser convergent angle:▲ - 30 °;◆ - 35 °; × - 40 °; ● - 45 °; ■ - 50 °.

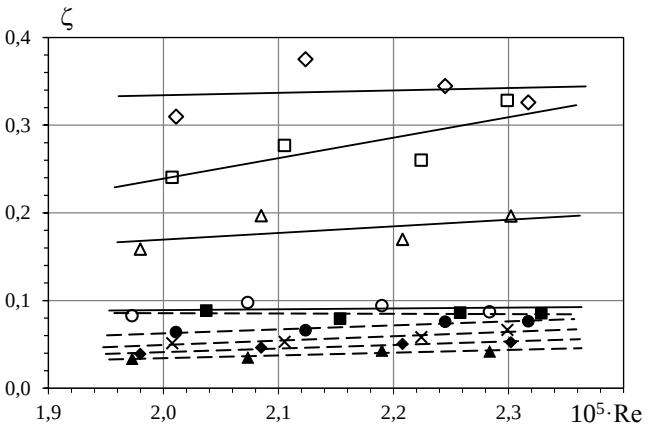

Figure 7 *– Dependence of local resistance coefficients ζ the average value of Re*

This equation (regression coefficient – R = 0.9857; R^2 = 0.9715) is obtained for the following flow characteristics of the confuser:

$$1.2 \cdot 10^5 < \mathrm{Re} < 3.4 \cdot 10^5;$$
$$\alpha = 30–50\ °;$$
$$M = 0.4–0.8;$$
$$n_c = 5.6–8.5.$$

The deviation of the calculated values of the coefficient ζ_c from those obtained in the numerical CFD simulation of $\zeta_{e.c}$ is $\delta_c = \pm 7$ % (Fig. 9).

Determining the local coefficient of resistance of the diffuser ζ_d is more difficult due to the influence of ambiguously interconnected geometric and operating parameters, the nature of the flow velocity field, and the prerequisites for the boundary layer separation phenomenon.

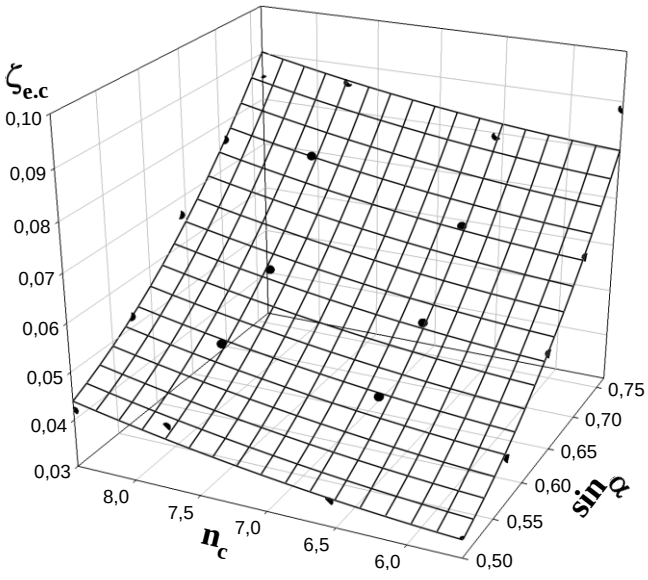

Figure 8 *– Dependence of the coefficient of local resistance of the confuser $\zeta_{e.c}$ on $\sin\alpha$ and contraction n_c ratio (distribution over the surface in accordance with equation (10, 11))*

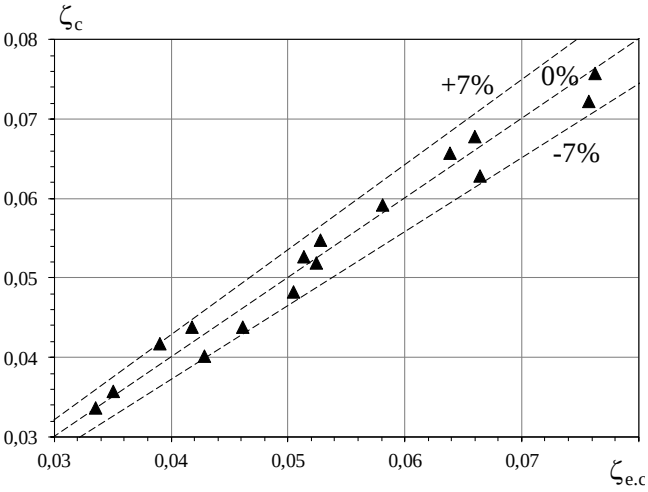

Figure 9 *– Comparison of experimental local resistance coefficients $\zeta_{e.c}$ in confuser with calculated ζ_c*

It should be noted that the prerequisites for the occurrence of the separation of the boundary layer occur in almost all modes of operation of the aerothermopressor. So, for example, when $M \geq 0.4$, additional flow turbulization occurs in the boundary layer of the diffuser (Fig. 10, a), at a diffuser divergent angle $\beta \geq 12$ ° (Fig. 10, b) the flow turbulization increases so that in the near-wall zone reverse air flow occurs. As a result, a flow separation occurs in the boundary layer (Fig. 11), which, in turn, leads to a sharp increase in the value of the local drag coefficient ζ_d.

Considering the above, the equation determination for the coefficient of local resistance of the diffuser ζ_d

was carried out by the method of approximation depending on the geometric parameters in accordance with a number of equations. In this case, the equations of a paraboloid of rotation were chosen (Fig. 12):

$$\zeta_d = \sin\beta\left(0.428 + 6.4174\sin\beta\right) + \\ + n_d\left(0.0142 - 7\cdot10^{-4}n_d\right) - 0.0794 \quad (12)$$

This equation (regression coefficient – R = 0.9828; R^2 = 0.9659) is obtained for the following flow characteristics of the diffuser:

$1.2 \cdot 10^5 < Re < 3.4 \cdot 10^5$;
β = 4-12 °;
α = 40 °;
M = 0.4-0.8;
n_d = 4.4–8.7.

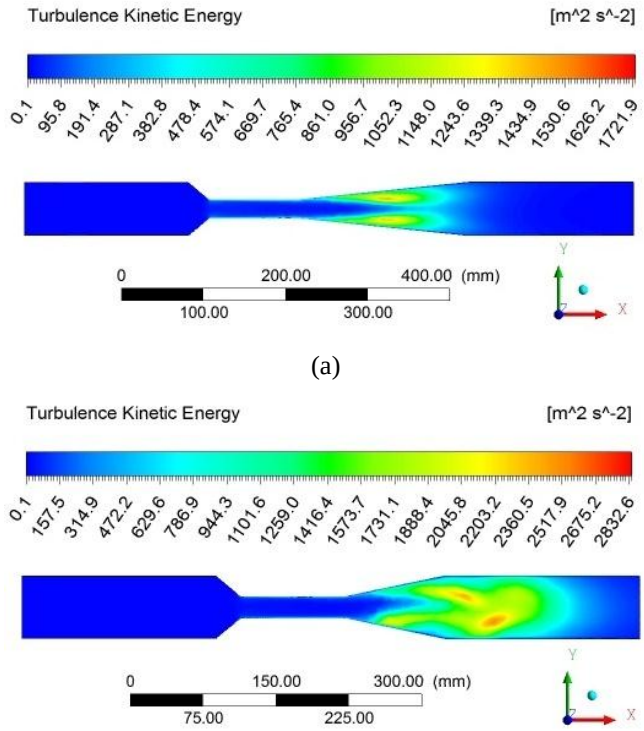

Figure 10 *– Turbulent kinetic energy distribution in the flow part of the aerothermopressor at a diffuser divergent angle* β = 6 ° *(a)* β = *12 ° (b) and M = 0.8*

The deviation of the calculated values of the coefficient ζ_d from those obtained in the numerical CFD simulation of $\zeta_{e.d}$ is δ_c = ± 10 % (Fig. 13).

When comparing the calculated data obtained by equation (12) with the experimental data obtained in [9, 17], one can see (Fig. 14) that the equation given for the diffuser gives a value with an allowable error (δ = ± 20 %) in the range of angles disclosures β = 6-12 °. At β = ≥ 12 °, the calculated values of ζ_d significantly exceed the experimental ones.

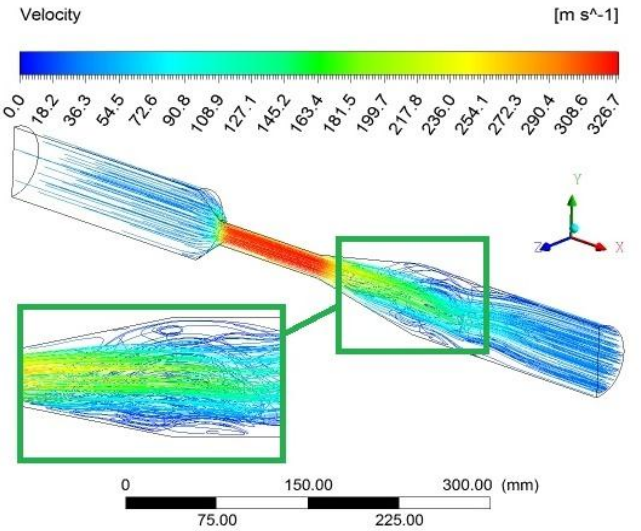

Figure 11 *– Streamlines of the air flow in the aerothermopressor at a diffuser divergent angle* β = *12 ° and M = 0.8*

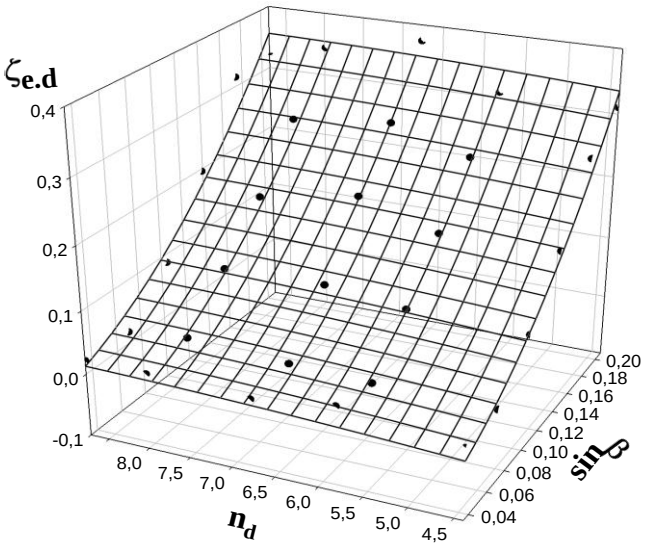

Figure 12 *– Dependence of the coefficient of local resistance of the diffuser $\zeta_{e.d}$ on sinβ and expansion n_d ratio (distribution over the surface in accordance with equation (12)*

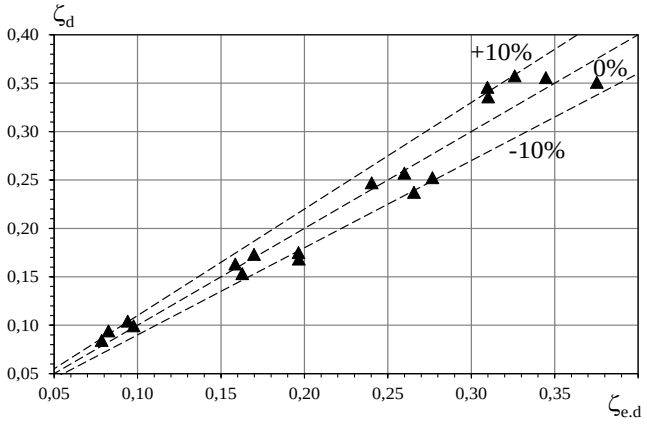

Figure 13 *– Comparison of experimental local resistance coefficients $\zeta_{e.d}$ in diffuser with calculated ζ_d*

The total pressure losses in the aerothermopressor due to the aerodynamic resistance are determined by the equation:

$$\Delta P_{loss}=\Delta P_l+\Delta P_{fr}=\left(\zeta_c+\zeta_d+\zeta_{fr}\frac{L_{ch}}{D_{ch}}\right)\frac{\rho w_{mix}^{\ 2}}{2}, \qquad (13)$$

w_{mix} – flow velocity in the working chamber;
ζ_c, ζ_d – coefficients of local resistance in the confuser and diffuser in accordance with the equations (11), (12); $\zeta_{fr} = \lambda_{fr}$ – coefficient of friction losses in the working chamber, which can be determined by Blausius [6, 8]:

$$\lambda_{fr}=\frac{0.3164}{Re^{0.25}}, \qquad (14)$$

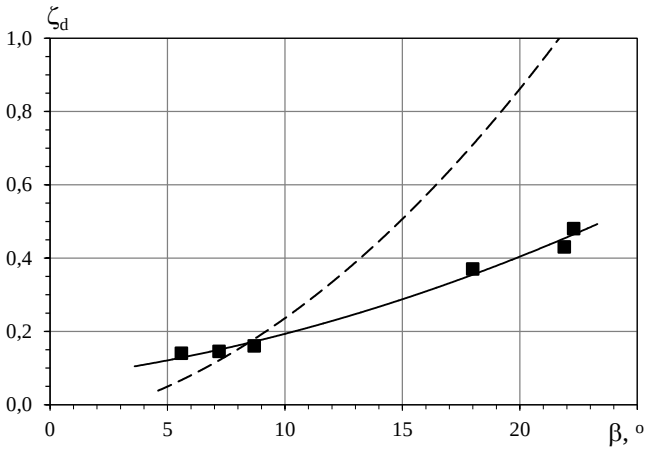

Figure 14 *– Comparison of the experimental coefficients of local resistances ζ_o in the diffuser with the calculated ones depending on the angle of taper β:*
_ _ _ _ - calculated curve according to equation (12)
■ - Experimental ζ_o with n_d = 4 and M = 0.4 according to the data given in [9, 17]

Analysis of the calculated data according to equation (14) shows that the total pressure loss in the "dry" aerothermopressor (without injection of liquid for evaporation) is ΔP_{loss} = 0.05-1.00·10^5 Pa (2-31%) at a fixed confuser convergent angle α = 40 ° and variable diffuser angle β = 4-14 ° (Fig. 15). At a fixed divergent angle of the diffuser β = 6 ° and variable angles of the confuser is α = 30-50 ° - ΔP_{loss} = 0.05-0.40·10^5 Pa (1-12%) (Fig. 16). It can be concluded that the effect of a change in the diffuser divergent angle is greater than the influence of the confuser convergent angle. At the same time, we can recommend angles α = 30 ° and β = 6 ° for the low-flow aerothermopressor, corresponding to the minimum pressure losses ΔP_{loss} = 1.0-9.5 %, and therefore to the maximum pressure increase as a result thermogasdynamic compression during injection and evaporation of fluid in the working chamber.

Numerical simulation to determine the total pressure losses in the aerothermopressor shows that with M = 0.6, α = 30 °, β = 6 ° - ΔP_{loss} = 0,2·10^5 Pa (6.6%) (Fig. 17). Thus, it can be seen that the calculated data fully correspond to the results of CFD modeling, and the obtained equations for determining the local resistance coefficients can be recommended for use in the low-flow aerothermopressor design method.

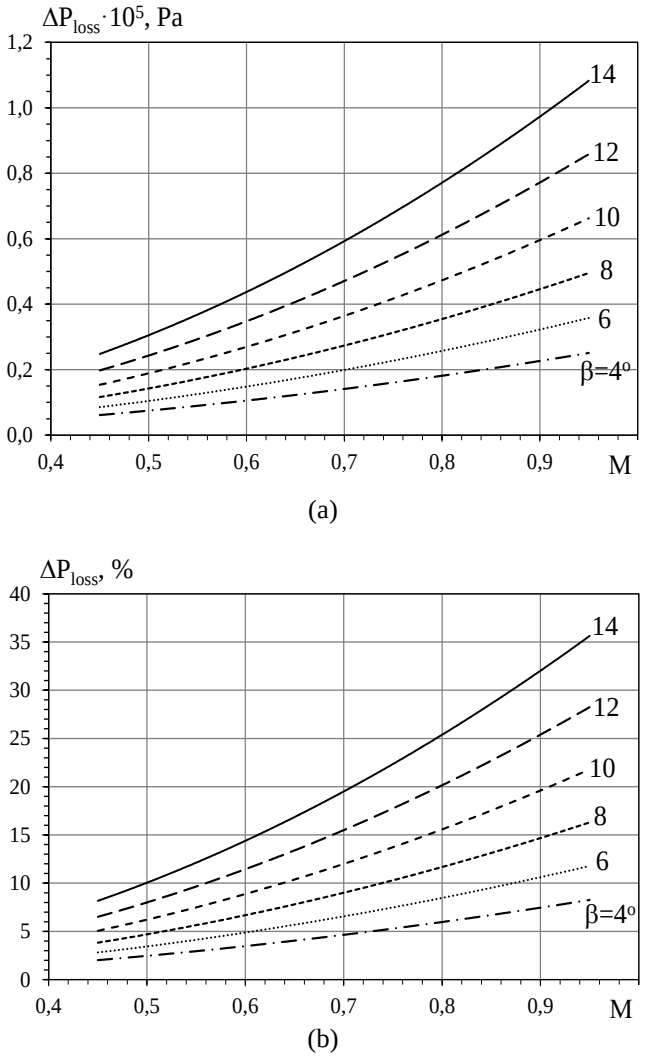

Figure 15 *– Dependences of total pressure loss ΔP_{loss} in the "dry" aerothermopressor in absolute (a) and relative (b) values on the air velocity M in the working chamber at different diffuser divergent angles β*

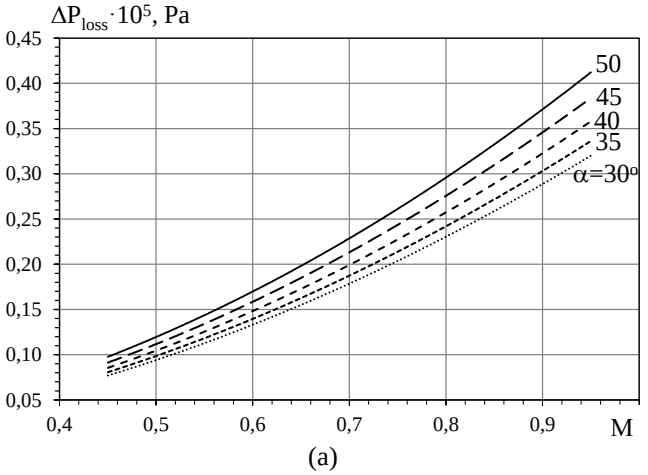

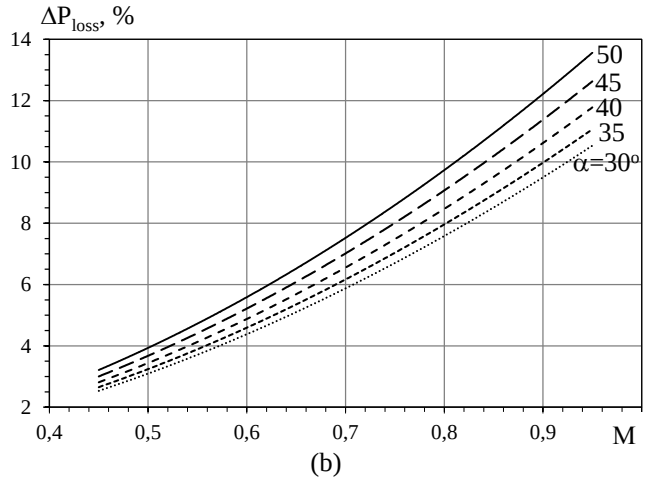

(b)

Figure 16 *– Dependences of total pressure loss ΔP_{loss} in the "dry" aerothermopressor in absolute (a) and relative (b) values on the air velocity M in the working chamber at different confuser convergent angles α*

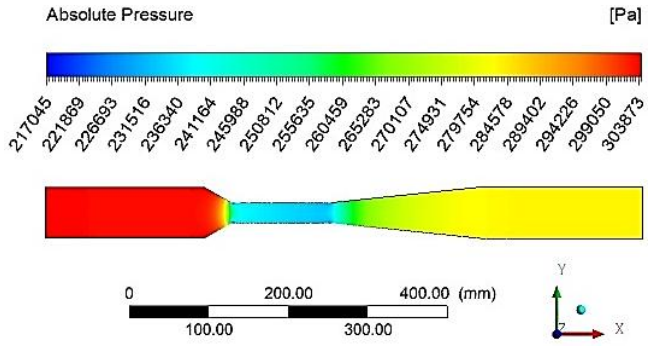

(a)

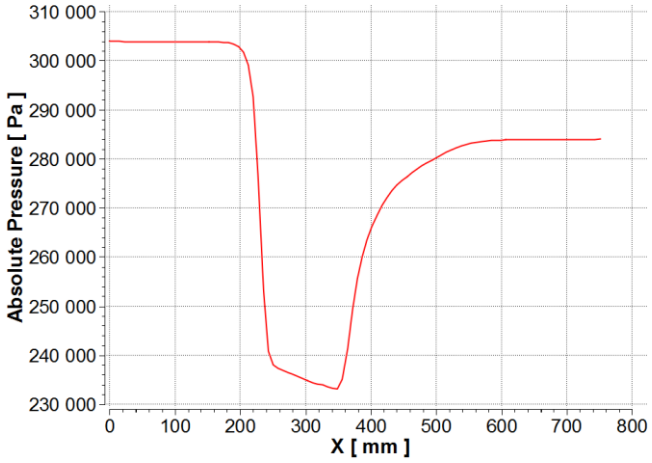

(b)

Figure 17 *– Absolute pressure P_a distributions of the air flow along the flow part length of the aerothermopressor: (a) – field distribution in the flow part; b) – pressure change P_a along the axis of the flow part*

5. Conclusions

1. The empirical equations for determining the coefficients of local resistance of the confuser ζ_c and diffuser ζ_d of the low-flow aerothermopressor are determined. The given results correspond to the following mode and geometrical characteristics $1.2 \cdot 10^5 < Re < 3.4 \cdot 10^5$; $\alpha = 30–50$ °; $\beta = 4\text{-}12$ °; M = 0.4–0.8; $n_c = 5.6–8.5$; $n_d = 4.4–8.7$.

2. The numerical values of local resistance coefficients was determined by using computer CFD modeling at M = 0.4–0.8: $\zeta_c = 0.02–0.08$ and $\zeta_d = 0.08–0.32$.

3. The recommended angles were determined: confuser convergent angle $\alpha = 30$ ° and diffuser divergent angle $\beta = 6$ °, corresponding to the minimum pressure loss $\Delta P_{loss} = 1.0–9.5$ %, and therefore also to the maximum pressure increase as a result of the thermogasdynamic compression that occurs during injection and evaporation of liquid in the working chamber.

References

1. **Konovalov D. V., Kobalava H. O.** (2018). Contact air cooling by using the aerothermopressor in the gas turbine plant cycle. *Refrigeration Engineering and Technology*. 54 (5), pp. 62-67. DOI: https://doi.org/10.15673/ret.v54i5.1248

2. **Konovalov D. V.** (2011). Termopresorni systemy okholodzhennia sudnovykh DVZ. *Aerospace Technic and Technology*. 10 (87), pp. 44-48. http://nti.khai.edu:57772/csp/nauchportal/Arhiv/AKTT/2011/AKTT1011/index.htm

3. **Zhivica V. I.** (2002). Promezhutochnye ohladiteli s termopressorom dlja dvuh stupenchatyh amiachnyh holodil'nyh ustanovok. *Holodil'naja tehnika*. 5, pp. 18-20.

4. **Stepanov I. R., Chudinov V. I.** (1977). Nekotoryie zadachi dvizheniya gaza i zhidkosti v kanalah i truboprovodah energoustanvok, Leningrad: Nauka. Leningradskoe otd., p. 199.

5. **Idelchik I. E.** (1975). Spravochnik po gidravlicheskim soprotivleniyam, Moskva: Mashinostroenie, p. 672.

6. **Kulinchenko V. R.** (2006). Hidravlika, hidravlichni mashyny i hidropryvid. Kyiv: "INKOS", Tsentr navchalnoi literatury, p. 616.

7. **Schmandt B., Herwig H.** (2011). Diffuser and Nozzle Design Optimization by Entropy Generation Minimization. *Entropy*. 13, pp. 1380-1402. doi:10.3390/e13071380

8. **Thevenin D., Janiga G.** (2014). Fluid Dynamics for Engineers. p. 272. http://www.uni-magdeburg.de/isut/LSS/Lehre/Vorlesungen/fluidmechDT_WWW.pdf

9. **Deych M. E., Zaryankin A. E.** (1970). Gazodinamika diffuzorov i vyhodnyh patrubkov turbomashin Moskva: Energiya, p. 384.

10. **Fowle A. A.** (1972). An experimental investigation of an aerothermopressor having a gas flow capacity of

25 pounds per second. Cambridge: Massachusetts Institute of Technolocy, p. 157.
11.**Konovalov D. V., Kobalava H. O.** (2018). Intercooling of the gas turbine plant cyclic air with an aerothermopressor. *Aerospace Technic and Technology*. 1 (145), pp. 29-36. http://nbuv.gov.ua/UJRN/aktit_2018_1_4
12.**ANSYS** Fluent Tutorial Guide Release 17.0. Canonsburg : ANSYS, Inc., 2016.
13.**Dvořák V., Novotny P., Dancova P.,Jasikova D.** (2012). PIV and CTA Measurement of Constant Area Mixing in Subsonic Air Ejector. *Experimental Fluid Mechanics*. 7 (1), pp. 109-114.
DOI: 10.1051/epjconf/20134501003
14.**Rao P. S., Moorthy C., Srinivas V.** (2017). Turbulence Modeling and Numerical Analysis for the Configuration of a Supersonic Air Ejector. *International Journal of Mechanical Engineering and Technology*. 8 (10), pp. 130-139. http://www.iaeme.com/IJMET/index.asp
15.**King Ch. D., Ölçmen S. M., Sharif M. A. R., Presdorf T.** (2013). Computational Analysis of Diffuser Performance for Subsonic Aerodynamic Research Laboratory Wind Tunnel. *Engineering Applications of Computational Fluid Mechanics*. 7 (4), pp. 419-432. DOI: 10.1080/19942060.2013.11015482
16.**Alvarenga, M. A., Andrade, C. R.** (2018). Compressible Subsonic Flow in Gas Turbine Annular Diffusers. *International Journal of Mathematical Models and Methods in Applied Sciences*. 12. pp. 159-166.
17.**Deych M. E.** (1974). Tehnicheskaja gazodinamika Moskva: Energoizdat, p. 592.

Received 24 January 2019
Approved 02 April 2019
Available in Internet 30 April 2019

Чисельне моделювання впливу режимних і геометричних характеристик на втрати тиску маловитратного аеротермопресора

Д. В. Коновалов, Г. О. Кобалава
Херсонська філія Національного університету кораблебудування імені адмірала Макарова,
пр. Ушакова, 44, м. Херсон, 73003, Україна

В роботі досліджуються гідрогазодинамічні процеси, які протікають в маловитратному аеротермопресорі. Цей струминний апарат представляє собою двофазовий струминний пристрій для контактного охолодження, в якому за рахунок відведення теплоти від газового потоку відбувається підвищення тиску газу та його охолодження (термогазодинамічна компресія). Високоефективна робота аеротермопресора залежить насамперед від конструкції проточної частини та способу розпилення води в апараті. Конструктивні чинники, які впливають на витрати енергії для подолання сил тертя та місцевих опорів на звужувально-розширювальних ділянках аеротермопресора, здійснюють значний вплив на робочі процеси в апараті. В роботі проведено дослідження ряду типових моделей аеротермопресора малої витрати із застосуванням комп'ютерного CFD-моделювання. Визначення основних параметрів потоку повітря (повний тиск, динамічний тиск, швидкість, температура та ін.) проводилося для ряду кутів конусності конфузора і дифузора, а також для ряду значень відносної швидкості повітря в робочій камері M = 0,4–0,8. Проведено порівняння отриманих даних з експериментальними. Відхилення розрахункових значень коефіцієнтів місцевих опорів в конфузові та в дифузорі від отриманих при комп'ютерному CFD-моделюванні не перевищує 7-10 %. Таким чином, отримано аналітичні залежності для визначення коефіцієнтів місцевого опору для конфузора (сопла) і дифузора, які можна рекомендувати для використання в методиці проектування аеротермопресорів малої витрати.

Ключові слова: *Аеротермопресор, Коефіцієнти Місцевих Опорів, CFD-моделювання*

Література

1. **Коновалов, Д. В., Кобалава, Г. О.** Застосування контактного охолодження повітря аеротермопресором в циклі газотурбінної установки [Текст] / Д. В. Коновалов, Г. О. Кобалава. // Холодильна техніка та технологія. – 2018. – № 54(5). – С. 62-67. DOI: https://doi.org/10.15673/ret.v54i5.1248
2. **Коновалов, Д. В.** Термопресорні системи охолодження суднових ДВЗ [Текст] / Д. В. Коновалов. // Авиационно-космическая техника и технология. – 2011. – №10 (87). – С. 44−48.
http://nti.khai.edu:57772/csp/nauchportal/Arhiv/AKTT/2011/AKTT1011/index.htm
3. **Живица, В. И.** Промежуточные охладители с термопрессором для двух ступенчатых амиачных

холодильных установок [Текст] / В. И. Живица. // Холодильная техника. – 2002. – №5. – С. 18−20.
4. **Степанов, И. Р.** Некоторые задачи движения газа и жидкости в каналах и трубопроводах энергоустановок [Текст] / И. Р. Степанов, В. И. Чудинов. – Ленинград: Наука. Ленингр. отд-ние, 1977. – 199 с. – (АН СССР, Кольск. филиал им. С.М. Кирова).
5. **Идельчик, И. Е.** Справочник по гидравлическим сопротивлениям [Текст] / И. Е. Идельчик. – Москва: Машиностроение, 1992. – 672 с.
6. **Кулінченко, В. Р.** Гідравліка, гідравлічні машини і гідропривід [Текст] / В. Р. Кулінченко. – Київ: Центр навчальної літератури, 2006. – 616 с.
7. **Schmandt, B., Herwig, H.** Diffuser and Nozzle Design Optimization by Entropy Generation Minimization [Text] / B. Schmandt, H. Herwig. // Entropy. – 2011. – no 13, P. 1380-1402.
DOI: 10.3390/e13071380
8. **Thevenin, D., Janiga, G.** Fluid Dynamics for Engineers [Text] / D. Thevenin, G. Janiga. // – 2014. – 272 p. http://www.unimagdeburg.de/isut/LSS/Lehre/Vorlesungen/fluidmechDT_WWW.pdf
9. **Дейч, М. Е., Зарянкин, А. Е.** Газодинамика диффузоров и выходных патрубков турбомашин [Текст] / М. Е. Дейч, А. Е. Зарянкин. // Москва: Энергия, 1970. – 384 р.
10. **Fowle, A. A.** An experimental investigation of an aerothermopressor having a gas flow capacity of 25 pounds per second [Text] / A. A Fowle. // Cambridge: Massachusetts Institute of Technolocy, 1972. – 157 p.
11. **Коновалов, Д. В., Кобалава, Г. О.** Проміжне охолодження циклового повітря в газотурбінних установках аеротермопресорами [Текст] / Д. В. Коновалов, Г. О. Кобалава. // Авіаційно-космічна техніка і технологія. – 2018. – № 1(145). – С. 29-36. http://nbuv.gov.ua/UJRN/aktit_2018_1_4
12. ANSYS Fluent Tutorial Guide Release 17.0. Canonsburg : ANSYS, Inc., – 2016.
13. **Dvořák, V., Novotny, P., Dancova, P.,Jasikova, D.** PIV and CTA Measurement of Constant Area Mixing in Subsonic Air Ejector [Text] / V. Dvořák, P. Novotny, P. Dancova, D. Jasikova. // Experimental Fluid Mechanics. – 2012. – no 7 (1). – P. 109-114. DOI: 10.1051/epjconf/20134501003
14. **Rao, P. S., Moorthy, C., Srinivas, V.** Turbulence Modeling and Numerical Analysis for the Configuration of a Supersonic Air Ejector [Text] / P. S. Rao, C. Moorthy, V. Srinivas. // International Journal of Mechanical Engineering and Technology. – 2017. – no 8(10). – P. 130-139.
http://www.iaeme.com/IJMET/index.asp
15. **King, Ch. D., Ölçmen, S. M., Sharif, M. A. R., Presdorf, T.** Computational Analysis of Diffuser Performance for Subsonic Aerodynamic Research Laboratory Wind Tunnel [Text] / Ch. D. King, S. M. Ölçmen, M. A. R. Sharif, T. Presdorf. // Engineering Applications of Computational Fluid Mechanics. – 2013. – vol. 7, no 4. – P. 419-432.
DOI: 10.1080/19942060.2013.11015482
16. **Alvarenga, M. A., Andrade, C. R.** Compressible Subsonic Flow in Gas Turbine Annular Diffusers [Text] / M. A. Alvarenga, C. R. Andrade. // International Journal of Mathematical Models and Methods in Applied Sciences. – 2018. – vol. 12. – P. 159-166.
17. **Дейч, М. Е.** Техническая газодинамика [Текст] / М. Е. Дейч // Москва: Энергоиздат, 1974. – 592 р.

Отримана в редакції 24.01.2019, прийнята до друку 02.04.2019